Aalborg Universitet

Investigation of heat transport across Ge/Si interface using an enhanced ballistic-diffusive model

Rezgui, Houssem; Nasri, Faouzi; Ben Aissa, Mohamed Fadhel; Blaabjerg, Frede; Belmabrouk, Hafedh; Guizani, Amen Allah

Accepted Manuscript

Investigation of heat transport across Ge/Si interface using an enhanced ballistic-diffusive model

Houssem Rezgui, Faouzi Nasri, Mohamed Fadhel Ben Aissa, Frede Blaabjerg, Hafedh Belmabrouk, Amen Allah Guizani
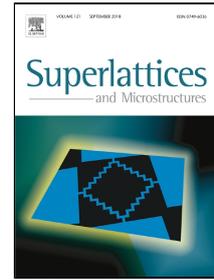
Please cite this article as: Houssem Rezgui, Faouzi Nasri, Mohamed Fadhel Ben Aissa, Frede Blaabjerg, Hafedh Belmabrouk, Amen Allah Guizani, Investigation of heat transport across Ge/Si interface using an enhanced ballistic-diffusive model, *Superlattices and Microstructures* (2018), doi: 10.1016/j.spmi.2018.09.018

Investigation of heat transport across Ge/Si interface using an enhanced ballistic-diffusive model

Houssem Rezgui[1,2]*, Faouzi Nasri [1], Mohamed Fadhel Ben Aissa[1], Frede Blaabjerg[3], Hafedh Belmabrouk[4], and Amen Allah Guizani[1,2]

[1]*Laboratory of Thermal Processes, Research and Technology Centre of Energy , Hammam Lif - Tunisia*

[2]University of Tunis El Manar, University Campus in Tunis, 2092, Manar II Tunis, Tunisia.

[3]Department of Energy Technology, Aalborg University, Aalborg 9220, Denmark.

[4]Laboratory of Electronics and Microelectronics, University of Monastir, Monastir 5019, Tunisia.

*Corresponding author

Email: houssem.rezgui@fst.utm.tn

Laboratory of Thermal Processes, Research and Technology Centre of Energy, P.B N°95, 2050 - Hammam Lif - Tunisia.

ABSTRACT

In this paper, we investigate the heat transport across Germanium-Silicon interface using an enhanced ballistic-diffusive equation (EBDE), where we introduce the temperature jump boundary condition coupled with a thermal boundary resistance (TBR) and an effective thermal conductivity model. This paper focuses on the thermal transport of sub-23 nm Ge/Si thin films. The present model is aimed to describe the ballistic-diffusive phonon transport across Ge/Si interface. We have found that the temperature jump occurs in the interface due to phonon-boundary interactions. In addition, the interfacial heat transport is influenced by the surface roughness effect. The prediction of the suggested EBDE model are in good accordance with analytical method reported in the literature. The proposed model shows excellent agreement with the phonon Boltzmann transport equation (BTE) approach and Monte Carlo simulation (MC). Further, the analytic model for the effective thermal conductivity (ETC) is in strong agreement with experimentally based approach and also the theoretical model.

KEYWORDS: Ballistic-diffusive heat transport; temperature jump condition; effective thermal conductivity; Ge/Si interface; surface roughness effect.

I. Introduction

Recent studies of heat transfer in nanoscale material have proved the important role of phonon transport at small scale [1–3]. Many theoretical and experimental methods have been developed to evaluate the nature of phonons scattering at surfaces and interfaces [4–9]. The heat transport across interfaces have an essential role in nanodevices, cooling of electronic circuits and engineering materials [10]. The thermal transport across Ge/Si based materials have been intensively reported owing to their application in transfer of energy. Ge/Si based nanomaterials can have low thermal conductivity, which is tremendously useful for

thermoelectric devices [11, 12]. Studying the Ge/Si interface plays a key role in the heat transport [1], Ge/Si core-shell nanowires [13–15] and also nanowire field-effect transistors (NWFETs) [16]. The classical heat conduction equation based on the Fourier law is unable to predict the phonons scattering mechanism. Most of nano-heat transport models are applied to investigate the nature of phonons interactions [17]. Tzou [18, 19] developed a heat conduction model given by the Dual-Phase-Lag model (DPL). The DPL model is used to describe the non-local effect in phonon systems. At nanostructure when the heat conduction passes through two different materials, a phenomenon of discontinuity in the temperature profile appears at the interface. This process is known as a temperature jump at the boundary (surface scattering) [20–26]. Nasri et al. [27] have evaluated the DPL model to report the heat transfer in nano-MOSFETs. They have applied the temperature jump boundary condition in the interface oxide-semiconductor. This process of temperature jump appears in the ballistic regime. Much research has focused on the ballistic-diffusive transport [28–35]. The aim of this proposed model is to predict the nano-heat transport at ultrafast time [29, 30] and describes the nature of phonon scattering at interfaces.

Recently, Rezgui et al. [28] have studied the BDE model to inquire the nano-heat transport in graphene nanoribbon field-effect transistor (GNRFET). They have predicted the phonon scattering mechanism in nano-transistors. Zhang and Ye [34] derived a modified BDE (MBDE) from the phonon BTE to model the non-continuum heat condition. It is found that this model is an efficient method to describe the temperature discontinuity at the boundary. Hua and Cao [22] have studied the phonon boundary scattering in nanofilms and they were using the Monte Carlo (MC) method to address the phonon transport at the boundaries.

In the present work, we have studied the nano-heat conduction across Ge/Si interface. We coupled the BDE model with the temperature jump boundary condition at the Ge/Si interface.

The proposed model characterizes the reduction of the thermal conductivity and describe the thermal transport between Ge and Si nanofilms. To better understand the nature of phonon transport, we have combined our predictive model with the TBR. Moreover, the temperature jump profile was compared with the MC simulation [22]. To validate the thermal conductivity, we have compared our suggested theoretical model with the results obtained from the literature [33] and experimental data [36–38].

II. Ballistic-diffusive equation

The phonon BTE, can be simplified with the gray relaxation-time approximation [28–30]

$$\frac{\partial f(r,v,t)}{\partial t} + v\nabla f(r,v,t) = -\frac{f - f_0}{\tau_R} \tag{1}$$

where f is the distribution function, f^0 is the equilibrium distribution function, v is the group velocity, and τ_R is the relaxation time related to resistive collision written as [34]:

$$\tau_R = \frac{3 \times k}{C \times v^2} \tag{2}$$

where κ is the thermal conductivity defined as:

$$\kappa = \frac{C \times v \times \Lambda}{3} \tag{3}$$

where Λ is the mean free path (MFP) written as $\Lambda = v\tau_R$ and C is the volumetric heat capacity [28, 34]. According to Matthiessen's rule [28, 35], the resistive relaxation time can be written as:

$$\frac{1}{\tau_R} = \frac{1}{\tau_u} + \frac{1}{\tau_i} + \frac{1}{\tau_b} \tag{4}$$

where τ_u is the relaxation time of umklapp phonon-phonon collisions, τ_i is the relaxation time of phonon-impurity collisions and τ_b is the relaxation time of phonon-boundary collision. The ballistic-diffusive approximation is to separate the distribution function into a ballistic

4

term f_b and a diffusive term f_m [28, 33, 34]. Olfe [39] proposed this approach to predict the radiation heat in a small system. The main idea of this approximation is to rewrite the distribution function in the following form [28, 34]

$$f = f_m + f_b \tag{5}$$

where f_b arises from the boundary scattering [34], defined as:

$$\frac{\partial f_b(r,v,t)}{\partial t} + v\nabla f_b(r,v,t) = -\frac{f_b}{\tau_R} \tag{6}$$

The second part is associated to the diffusive component f_m and denotes the scattering mechanism in internal point inside the domain. The fundamental equation for f_m is defined as [28, 34]:

$$\frac{\partial f_m(r,v,t)}{\partial t} + v\nabla f_m(r,v,t) = -\frac{f_m - f_0}{\tau_R} \tag{7}$$

We can define the diffusive flux [28, 35] as:

$$q_m(t,r) = \int_\varepsilon v(r,t) f_m(r,\varepsilon,t)\varepsilon\, \mathrm{D}(\varepsilon) d\varepsilon \tag{8}$$

where ε is the kinetic energy and $D(\varepsilon)$ is the density of states. By using the first order Taylor expansion of Eq. (7) and assuming that $\Delta t = \tau_R$, we can obtain [35, 40]:

$$\frac{f_m(r,\varepsilon(v),t+\tau_R) - f_m(r,\varepsilon(v),t)}{\tau_R} + v\nabla f_m(r,\varepsilon(v),t) = -\frac{f_m(r,\varepsilon(v),t) - f_0(r,\varepsilon(v))}{\tau_R} \tag{9}$$

By rearranging the terms of Eq. (9) we may obtain

$$f_0(r,\varepsilon(v)) = \tau_R v\nabla f_m(r,\varepsilon(v),t) + f_m(r,\varepsilon(v),t+\tau_R) \tag{10}$$

Multiplying Eq. (10) with $\varepsilon\, \mathrm{D}(\varepsilon)v$ and using $\int_\varepsilon f_0\varepsilon\, \mathrm{D}(\varepsilon)vd\varepsilon = 0$, we can conclude that:

$$q_m(r,t+\tau_R) + \int_\varepsilon \tau_R v\nabla f_m(r,\varepsilon(v),t)\varepsilon\, \mathrm{D}(\varepsilon)vd\varepsilon = 0 \tag{11}$$

5

Assuming that $\nabla f = \dfrac{df}{dT}\nabla T$, Eq. (11) becomes [35]:

$$q_m(r, t + \tau_R) = -\kappa \nabla T_m(r,t) \tag{12}$$

where κ is the thermal conductivity defined as $\kappa = \int \tau_R v^2 \dfrac{df_m}{dT}\varepsilon\, \mathrm{D}(\varepsilon)d\varepsilon$

The derivation of Eq. (12) leads to the following equation

$$\tau_R \frac{\partial q_m(r,t)}{\partial t} + q_m(r,t) = -\kappa \nabla T_m(r,t) \tag{13}$$

where T_m is the temperature related to the diffusive part [34].

For the Ballistic part, the heat flux is written as [28]:

$$q_b(t,r) = \int_\varepsilon v(r,t) f_b(r,\varepsilon,t)\varepsilon\, \mathrm{D}(\varepsilon)d\varepsilon \tag{14}$$

The total internal energy is defined as [28]:

$$\mathrm{u}(r,t) = u_b(r,t) + u_m(r,t) \tag{15}$$

where $u_b(r,t)$ and $u_m(r,t)$ are the internal energy of the ballistic and the diffusive component respectively. By using Eq. (6) and the similar derivation of Eq. (7) we can obtain

$$\tau_R \frac{\partial u_b(r,t)}{\partial t} + u_b(r,t) = -\tau_R \times \nabla.q_b(r,t) \tag{16}$$

The energy conservation is defined as:

$$-\nabla.q(r,t) + \dot{q}_h = \frac{\partial u(r,t)}{\partial t} = C\frac{\partial T(r,t)}{\partial t} \tag{17}$$

where $\dot{q}_h$ is the volumetric heat generation and q is the total heat flux [28]. The total heat flux is expressed as

$$q(t,r) = q_b(t,r) + q_m(t,r) \tag{18}$$

6

Substituting Eq. (13) and Eq. (16) into Eq. (17), we can obtain the ballistic-diffusive equation [28, 34]:

$$\tau_R \frac{\partial^2 T_m(r,t)}{\partial t^2} + \frac{\partial T_m(r,t)}{\partial t} = \frac{1}{C}\nabla(\kappa\nabla T_m(r,t)) - \frac{1}{C}\nabla q_b(r,t) + \frac{\dot{q}_h}{C} + \frac{\tau_R}{C}\frac{\partial \dot{q}_h}{\partial t} \tag{19}$$

Note that Eq. (19) denotes the original BDE model where κ is bulk thermal conductivity. However, according to our suggested EBDE model, the thermal conductivity is replaced by an effective one (apparent thermal conductivity) where we introduce the specularity parameter which will be discussed later.

III.   Effective thermal conductivity of nanofilms

The thermal conductivity is reduced by many effects such as boundary scattering, non-local effects and geometries. For the thermal transport of nanostructures in contact with two different temperatures, phonons are emitted from the heat sink at the boundary [7, 41]. Hence, the variation of effective thermal conductivity is affected by phonon-boundary scattering and thermal resistance [7, 22, 23]. In nanofilms (lengths are comparable to phonon MFP), the heat transport is limited by the ballistic transport, which is characterized by the increase of the Knudsen number [22, 41]. For large Knudsen number, phonon-boundary scattering dominate the resistive mechanism (Casimir limit) [22, 42, 43]. Across the nanostructure, phonons are traveling ballistically (from boundary to boundary) as it is shown in Fig. 1. Furthermore, when boundary scattering dominate due to the ballistic nature of heat transport, normal collision scattering supposed negligible [42, 44]. In this work, we are suggesting a theoretical model for the ETC, which is given by [28, 45, 46]:

$$k_{eff}(Kn) = \kappa\left[1 - \frac{2Kn \times \tanh(1/2Kn)}{1 + C_W \times \tanh(1/2Kn)}\right] \tag{20}$$

where $Kn = \dfrac{\Lambda}{L}$ is the Knudsen number, L is the nanostructure length, $C_W = 2\left(\dfrac{1+p}{1-p}\right)$ is a constant related to the properties of the walls [45, 46] and p is the specularity parameter defined as the probability of phonon reflection at the surface scattering [6–8, 45].

For high Kn values, phonon-interface effects reduces the thermal conductivity. Eq. (20) predicts the ETC and leads to [28, 45]:

$$\kappa_{eff}(Kn) = \kappa\left(\frac{C_W}{2Kn}\right) \tag{21}$$

In this work, the enhanced ballistic-diffusive equation (EBDE) model is rewritten as [28]:

$$\tau_b \frac{\partial^2 T_m(r,t)}{\partial t^2} + \frac{\partial T_m(r,t)}{\partial t} = \frac{\kappa_{eff}}{C}\nabla\nabla T_m(r,t) - \frac{\nabla q_b(r,t)}{C} + \frac{\dot{q}_h}{C} + \frac{\tau_b}{C}\frac{\partial \dot{q}_h}{\partial t} \tag{22}$$

We introduce a new approach for the relaxation time associated to the phonon boundary scattering which is defined as:

$$\tau_b = \frac{3\times\kappa_{eff}}{C\times v^2} \tag{23}$$

By replacing Eq. (21) into Eq. (23), we can obtain the Ziman formula [28, 47]:

$$\frac{1}{\tau_b} = \left(\frac{1-p}{1+p}\right)\times\left(\frac{v}{L}\right) \tag{24}$$

where $\dfrac{1}{\tau_b}$ is the phonon scattering rate.

When the phonon MFP is longer than the characteristic length of the system, thermal transport is predominated by phonon-boundary scattering [22, 43]. In our case, the thermal conductivity depends on the size of nanostructure and the group velocity. The phonon-boundary interactions can be determined by the Callaway's model [48], which is based on a simple boundary scattering rate which is given by the following expression:

$$\frac{1}{\tau_b} = \frac{v}{L} \tag{25}$$

8

IV. Temperature jump boundary condition

The temperature jump phenomena that is given by a discontinuity process appears in the surface scattering between two materials. In addition, the temperature jump occurs due to the ballistic transport and phonons-interfaces collisions [22]. In fact, in the diffusive regime (Kn<<1), such discontinuous process is assumed to be negligible. Criado-Sancho and Jou [24] have analyzed the heat transfer between Si and Ge materials, and they derived a temperature profile written as:

$$T_{Si} - T_{Ge} = R \times q \tag{26}$$

where q is the heat flux travel from Si side to Ge side and R is thermal boundary resistance. In recent work, Rezgui et al. [49], have studied the heat dissipation in a nanoscale MOSFET. The temperature jump boundary condition is defined as

$$T - T_W = -d \times Kn \times L \times \frac{\partial T}{\partial x} \tag{27}$$

where T_W is the wall temperature and d is an adjustable coefficient related to the properties of materials. To better predict phonon transport in naostructures, Ben aissa et al. [21] have defined and calculated the adjustable coefficient d which is given by the following expression:

$$d = \frac{R \times \kappa_{eff}}{Kn \times L} \tag{28}$$

In a similar work, Hua and Cao [22] have used the MC technique to investigate the phonon transport across nanofilms, where they have proposed a temperature jump boundary condition which is written as:

$$T - T_W = -\frac{2}{3} \times \Lambda \times \frac{\partial T}{\partial x} \tag{29}$$

The work of Guo and Wang [20] has proved that the temperature jump boundary condition for the phonon hydrodynamic model can be established as:

9

$$T - T_W = -\frac{2}{3} \times \frac{1+p}{1-p} \Lambda \times \frac{\partial T}{\partial x} \tag{30}$$

At the interface scattering, the temperature gradient is equivalent to the wall temperature gradient [21]:

$$\frac{\partial T}{\partial x} = \frac{\partial T_W}{\partial x} \tag{31}$$

In the ballistic regime, the temperature gradient into the nanofilms decreases, while the temperature jump appears at the interface [50]. In this case, we can define the heat flux in the form of Fourier's law [41, 50]:

$$q = \kappa_{eff} \times \frac{\Delta T}{L} \tag{32}$$

where $\Delta T = T_h - T_c$, T_h and T_c represents the hot and cold source respectively. According to Eq. (31), the energy conservation leads to the following equation:

$$\frac{\partial q_x}{\partial x} = 0 \, .$$

The temperature differential equation is given by:

$$\frac{d^2 T}{dx^2} = 0 \tag{33}$$

The general solution of Eq. (33) is $T(x) = Ax + B$, where A and B are two positive constants. Hence, the initial conditions are expressed as:

$$\frac{\partial T_W}{\partial x} = A \, , \; T(x = 0) = B$$

The following dimensionless variables were introduced to solve the non-dimensional temperature distribution:

$$T^* = \frac{T - T_C}{T_h - T_c} \, , \; X^* = \frac{x}{L} \, , \; Y^* = \frac{y}{L} \, , \; q^* = \frac{q}{C v_g (T_h - T_c)} \, , \; t^* = \frac{t}{\tau_R}$$

According to Eq. (27), we have defined the temperature jump at the interface.

For X= 0, Eq. (27) gives

$$T_h - T = -d \times \Lambda \times \frac{\partial T}{\partial x} \tag{34}$$

For X= L, Eq. (27) is rewritten as

$$T - T_c = -d \times \Lambda \times \frac{\partial T}{\partial x} \tag{35}$$

Substituting Eq. (34) and Eq. (35) into $T(x)$, we can obtain the following temperature profile

$$T^* = \frac{(1+(d \times Kn)) - X^*}{(1+(2 \times d \times Kn))} \tag{36}$$

In this work, the temperature jump boundary condition at the interface depends on the Knudsen number, the thermal boundary resistance and the specularity parameter p. The use of the parameter d is aimed to better predict the heat transport across the interfaces.

V. Structures to model

In order to validate our proposed model, the EBDE model is solved for two-dimensional (2D) heat conduction problems. The 2D rectangular domain system has the following geometries:

L_x = 100 nm, L_y = 50 nm, L= L_h= 10 nm.

where L_h is the heater region length. More details are shown in Fig. 2 and Refs. [2, 34]. The second structure shown in Fig. 3(a) serves to consider the Ge/Si interface. This geometry consists of a single crystalline Ge covered by a Si layer [22]. Fig. 3(b) depicts the mechanism of scattering at the surface roughness, where the dimension of the nanostructure is extracted from the literature [14]. In the present work, the Ge substrate thickness is fixed at L_{Ge} = 20 nm, the Si nanofilm thickness is fixed at L_{Si} =3 nm and the interface length is L = L_y= 20 nm. Our proposed structure has the same geometries given by Hua and Cao [22]. The right and left side are supposed to be adiabatic. Due to phonon-wall collision, the Ge/Si interface is exposed to the temperature jump boundary conditions. During our simulations, the thermal boundary

resistance is $R_{Ge-Si}=5.76 \cdot 10^{-9}$ Km^2W^{-1} [51] and T_{ref} is the reference temperature ($T_{ref}=300$ K).

To compute the EBDE model coupled with the temperature jump boundary condition we use

the finite element method (FEM) [49]. The FEM method was a good argument to study the

phonon transport in 2D domains [32, 49]. The materials involved in the numerical study are

Silicon (Si) and Germanium (Ge) [22] and they are listed in Table I.

VI.   Results and discussion

A. Verification of theoretical model

In this work, we study the heat transfer across Ge/Si interface. First, we demonstrate our

proposed model for the ETC. Our results are compared with others numerical work [33] and

experimental data [36–38].

Fig. 4 shows the reduction of the ETC versus the Knudsen number. It is clear that the ETC

decreases when the Knudsen number increases. For small value of Kn, it is found that, Eq.

(20) for p= 0.5 is in good agreement with data obtained by Hua and Cao [33] and the

experimental data [36, 37]. For a high Knudsen number, our proposed model is in agreement

with the experimental data obtained by Liu and Asheghi [38]. The ETC varied from 12~20%

when the specularity is ranging from p= 0.3 to p=0.5. It can be seen that the ETC shows a

strong dependence with the Knudsen number. Fig. 5 illustrates the size-dependent thermal

conductivity of crystalline C-Ge and C-Si. It is obvious that our theoretical model accords

with data obtained in Ref. [51]. From this figure, we show the strong reliance of the thermal

conductivity within the length of nanostructure.

Additionally, the thermal conductivity depends on the TBR, which is defined as; $R = \dfrac{L}{k}$ [22,

51]. Alvarez and Jou [52] noted that the TBR arises from the discontinuity of the temperature

at the interfaces. To predict the temperature distribution at the boundary, we use Eq. (27). Fig.

6 shows an excellent agreement between our proposed model and the MC simulation given by Hua and Cao [22]. The classical Fourier's law is applied only for small values of the Knudsen number, which denotes that the Fourier heat equation cannot predict the thermal transport in nanoscale regime. The increase of the Knudsen number is manifested by the increase of the temperature at the boundary. For small value of Knudsen number, a fully diffusive regime dominate the thermal transport. In this case, the temperature jump vanishes and the classical heat equation can be employed [32, 50].

B. Validation of the EBDE model

To validate our suggested EBDE model associated with the temperature jump boundary condition, we have compared our results with BTE, MBDE model [34] and the classical BDE model. In this case we verify our present EBDE model for Kn= 1. Fig. 7 shows the non-dimensional temperature and heat flux along y-axis in the centerline ($x=L_x/2$) at $t^*=10$ and Kn= 1. It is evident that our proposed EBDE model predicts the decrease of the temperature and the heat flux similar to the BTE and the MBDE given by Zhang and Ye. [34]. The temperature is maximal in the heater zone and reduced to the ambient when we pass to the coldest side. Fig. 8 shows the temperature and the heat flux distribution along the line Y= 0 at $t^*= 1$ and Kn= 1. It can be seen that our EBDE model capture the increase of the interfacial heat transport near to the BTE. The new temperature boundary condition given by Eq. (27) coupled with EBDE model leads to more improvement especially at the interface. At the boundary, the temperature profile is affected by the nature of phonon scattering [7, 22]. In this side, the EBDE model is much more accurate than the original BDE. Fig. 9 shows the temperature and the heat flux profiles for Kn= 10 at ultrafast time scale $t^*= 0.1$. When phonons are scattered across interfaces, such temperature jump arises near the boundary. Therefore, the phonons collision process give rise to the perturbation in the temperature and heat flux curve as shown in Fig. 10.

13

Fig. 8 and Fig. 10 have clearly explained that the heat transport depend on the variation of the Knudsen number. The temperature jump occurs at the interface, which is related to phonon interaction. For Kn= 1, we shows a strong deviation in the temperature and heat flux curve because of the frequent phonon interactions. In the ballistic regime (Kn= 10), the interactions between phonons are reduced and a weak deviation is shown in the heat flux profile. Our present EBDE model has successfully predicted the transition of heat transport. In addition, the prediction of our model is in good accordance with the BTE results.

C. Heat transfer across Ge/Si interface

In this case, we investigate the heat transport at the interface Ge/Si. In order to consider the 2D geometry, the results are presented along the line X= 0 at time t= 50 ps. Fig. 11 represents the temporal evolution of the temperature calculated using the EBDE model. It is clear that the temperature reaches the peak values at the interface Ge/Si. For a short time (10 ps), the temperature achieved is 317.4 K. For 20 ps and 30 ps, the temperature reaches respectively 326.7 K and 327.6 K. The saturation of the temperature is appearing at L= 20 nm (interface scattering). The temperature jump is located at hot surfaces, where phonons interactions are frequent [32]. Hence, the TBR occurs at the boundary due to the phonons scattering effect and the variation of the thermal conductivity [22].

Fig. 12 depicts the temperature distribution along x-y plane using the EBDE for p= 0.2, p= 0.3, and p= 0.4. It is found that the temperature reaches 311.4 K for p=0.4 and 321.8 for p= 0.2. For specular surfaces scattering, the temperature jump is reduced due to the increase of the thermal conductivity. The temperature distribution shows a strong relation with the phonon interactions at the interface. Referring to the diffusive mismatch model (DMM), the phonon transport is purely diffusive (maximum of phonons interactions) at interfaces [25]. Fig. 13 shows the evolution of heat flux across the interface Ge/Si at t= 5ps with different

specularity p= 0.1, p= 0.3 and p= 0.5. It is obvious that the heat flux obtains the maximum in the Ge/Si interface. For diffuse surface (p= 0.1), the heat flux reaches 34.7 (10^9 W/m^2). However, for a smooth surface (p= 0.5) the heat flux decreases and attaints 22.8 (10^9 W/m^2). The heat conduction across the interfaces depends on essential properties [7]: (1) Nature of phonon-surface interactions (specular or diffuse surface), (2) the variation of the thermal conductivity and (3) the thermal boundary resistance at interface scattering.

To reduce the heat flux and the peak temperature across the interfaces, it is necessary to increase the specularity parameter. The work of Li and McGaughey [7] prove that emitted phonons have a specular reflection (p≈ 1) which lead to an excellent quality interface. Experimental studies have demonstrated that the edge roughness of graphene ribbons was characterized by higher specularity parameter (p > 0.5) [53], which is implying that graphene-based materials are needed in the future organic electronic devices. Due to their environmental safety, graphene-like materials are implemented in various application such as, green technologies [54], 2D flexible nanoelectronics [55] and manufacturing of novel biointerfaces [56].

VII. Conclusion

In summary, we have developed an enhanced ballistic-diffusive equation (EBDE) derived from the phonon Boltzmann transport equation. By including a new boundary condition, the EBDE becomes more appropriate and is able to predict the heat transport across interfaces. In addition, the theoretical thermal conductivity model agrees with the results obtained from the literature and experimental data. It is found that the temperature jump at the boundary was manifested by the variation of the thermal conductivity and the thermal boundary resistance. Moreover, our proposed temperature boundary condition is in good agreement with the MC simulation. It is also found that heat transport across interfaces depends on the properties of

the phonon-surface roughness. Due to the growing needs of organic-based materials, we intend to investigate the heat transport in the Graphene-Silicon interface in the future. In addition, we will develop another model based on the phonons hydrodynamics model where the phonon normal scattering has an essential role in the heat transport [20, 45, 57].

Acknowledgements

References

[1] X. Ran, Y. Guo, M. Wang, Interfacial phonon transport with frequency-dependent transmissivity by Monte Carlo simulation, Int. J. of Heat and Mass Trans. 123 (2018) 616–628. DOI: https://doi.org/10.1016/j.ijheatmasstransfer.2018.02.117.

[2] C. Zhang, Z. Guo, S. Chen, Unified implicit kinetic scheme for steady Multiscale heat based on the Boltzmann transport equation, Phys. Rev. E 96 (6) (2017) 063311. DOI: 10.1103/PhysRevE.96.063311.

[3] H.L. Li, Y.C. Hua, B.Y. Cao, A hybrid phonon Monte Carlo-diffusion method for ballistic-diffusive heat conduction in nano- and micro- structures, Int. J. of Heat and Mass Trans. 127 (2018) 1014–1022. DOI: https://doi.org/10.1016/j.ijheatmasstransfer.2018.06.080.

[4] M. Mahdouani, R. Bourguiga, Auger and carrier-surface phonon interaction processes in graphene on a substrate made of polar materials, Superlattices and Microstructures 102 (2017) 212–220. DOI: https://doi.org/10.1016/j.spmi.2016.12.043.

[5] W. Chen, J. Yang, Z. Wei, C. Liu, K. Bi, D. Xu, D. Li, Y. Chen, Effects of interfacial roughness on phonon transport in bilayer silicon thin films, Phys. Rev. B 92 (13) (2015) 134113. DOI: 10.1103/PhysRevB.92.134113.

[6] K. Kothari, M. Maldovan, Phonon surface scattering and thermal energy distribution in superlattices, Sci. Rep. 7 (2017) 5625. DOI: 10.1038/s41598-017-05631-3.

[7] D. Li, A. J. H. McGaughey, Phonon dynamics at surfaces and interfaces and its implications in energy transport in nanostructured materilas–An opinion paper, Nanoscale Microsc. Thermophys. Eng. 19 (3) (2015) 166–182. DOI: https://doi.org/10.1080/15567265.2015.1035199.

[8] A. Malhotra, M. Maldovan, Impact of phonon surface scattering on thermal energy distribution of Si and SiGe nanowires, Sci. Rep. 6 (2016) 25818. DOI: 10.1038/srep25818.

[9] F. Ruffino, M.G. Grimaldi, Roughness evolution in dewetted Ag and Pt nanoscale films, Superlattices and Microstructures 113 (2018) 430–441. DOI: https://doi.org/10.1016/j.spmi.2017.11.033.

[10] J. Xiang, W. Lu, Y. Hu, Y. Wu, H. Yan, C.M. Lieber, Ge/Si nanowires heterostructures as high-performance field-effect transistors, Nature (London), 441 (2006) 489–493. DOI: 10.1038/nature04796.

[11] X. Mu, L. Wang, X. Yang, P. Zhang, A.C. To, T. Luo, Ultra-low thermal conductivity in Si/Ge hierarchical superlattice nanowire, Sci. Rep. 5 (2015) 16697. DOI: 10.1038/srep16697.

[12]   X. Chen, Z. Wang, Y. Ma, Atomistic design of high thermoelectricity on Si/Ge superlattice nanowires, J. Phys. Chem. C, 115 (42) (2011) 20696–20702. DOI: 10.1021/jp2060014.

[13]   M. Hu, K.P. Giapis, J.V. Goicochea, X. Zhang, and D. Poulikakos, Significant reduction of thermal conductivity in Si/Ge core–Shell nanowires, Nano Lett. 11 (2) (2011) 618–623. DOI: 10.1021/nl103718a.

[14]   M.C. Wingert, Z.C.Y. Chen, E. Dechaumphai, J. Moon, J.H. Kim, J. Xiang, R. Chen, Thermal conductivity of Ge and Ge–Si core–shell nanowires in the phonon confinement regime, Nano Lett. 11 (12) (2011) 5507–5513. DOI: 10.1021/nl203356h.

[15]   B.M. Nguyen, Y. Taur, S.T. Picraux, S.A. Dayeh, Diameter-independent hole mobility in Ge/Si core/shell nanowire field effect transistors, Nano Lett. 14 (2) (2014) 585–591. DOI: 10.1021/nl4037559.

[16]   G. Liang, J. Xiang, N. Kharche, G. Klimeck, C.M. Lieber, M. Lundstrom, Performance analysis of Ge/Si core/Shell nanowire field-effect transistor, Nano Lett. 7 (3) (2007) 642–646. DOI: 10.1021/nl062596f.

[17]   J.B. Hertzberg, M. Aksit, O.O. Otelaja, D.A. Stewart, R.D. Robinson, Direct measurements of surface scattering in Si nanosheets using a microscale phonon spectrometer: Implication for Casimir-limit, Nano Lett. 14 (2) (2014) 403–415. DOI: 10.1021/nl402701a.

[18]   D.Y. Tzou, Nonlocal behavior in thermal lagging, Int. J. of Therm. Sci. 49, (7) (2010) 1133–1137. DOI: https://doi.org/10.1016/j.ijthermalsci.2010.01.022.

[19]   D.Y. Tzou, Nonlocal behavior in phonon transport, Int. J. of Heat and Mass Trans. 54 (2011) 475–481. DOI: https://doi.org/10.1016/j.ijheatmasstransfer.2010.09.022.

[20]   Y. Guo, M. Wang, Phonon hydrodynamics for nanoscale heat transport at ordinary temperatures, Phys. Rev. B 97 (2018) 035421. DOI: 10.1103/PhysRevB.97.035421.

[21]   M.F. Ben Aissa, F. Nasri, H. Belmabrouk, Multidimensional Nano Heat Conduction in Cylindrical Transistors, IEEE Trans. Electron Devices 64 (12) (2017) 5236–5241. DOI: 10.1109/TED.2017.2763241.

[22]   Y.C. Hua, B.Y. Cao, Slip Boundary Conditions in Ballistic-Diffusive Heat Transport in Nanostructures, Nanoscale and Microsc. Thermophys. Eng. 21 (3) (2017) 159–176. DOI: https://doi.org/10.1080/15567265.2017.1344752.

[23]   J. Kaiser, T. Feng, J. Maassen, X. Wang, X. Ruan, M. Lundstrom, Thermal transport at the nanoscale: A Fourier's law Vs. phonon Boltzmann equation study, J. Appl. Phys. 121 (4) (2017) 044302. DOI: https://doi.org/10.1063/1.4974872.

[24]   M. Criado-Sancho, D. Jou, A simple model of thermoelastic heat switches and heat transistors, J. Appl. Phys. 121 (2) (2017) 024503. DOI: https://doi.org/10.1063/1.4974011.

[25]   X. Ran, Y. Guo, M. Wang, Interfacial phonon transport through Si/Ge multilayer film using Monte Carlo scheme with spectral transmissivity, Front. Energy Res. 6 (28) (2018). DOI: 10.3389/fenrg.2018.00028.

[26]   K. Alaili, J. Ordonez-Miranda, Y. Ezzahri, Effective interface thermal resistance and thermal conductivity of dielectric nanolayers, Int. J. of Therm. Sci. 131 (2018) 40–47. [Online]. Available: https://doi.org/10.1016/j.ijthermalsci.2018.05.024.

[27]   F. Nasri, M.F. Ben Aissa, H. Belmabrouk, Nanoheat Conduction Performance of Black Phosphorus Filed-Effect Transistor, IEEE Trans. Electron Devices, 64 (6) (2017) 2765–2769. DOI: 10.1109/TED.2017.2694484.

[28]   H. Rezgui, F. Nasri, M.F. Ben Aissa, H. Belmabrouk, A.A. Guizani, Modeling Thermal Performance of Nano-GNRFET Transistor Using Ballistic-Diffusive Equation, IEEE Trans. Electron Devices, 65 (4) (2018) 1611–1616. DOI: 10.1109/TED.2018.2805343.

[29]   D.S. Tang, B.Y. Cao, Ballistic thermal wave propagation along nanowires modeled using phonon Monte Carlo simulations, App. Therm. Eng. 117 (2017) 609–616. DOI: https://doi.org/10.1016/j.applthermaleng.2017.02.078.

[30]   D.S. Tang, Y.C. Hua, B.Y. Cao, Thermal wave propagation through nanofilms in ballistic-diffusive regime by Monte Carlo simulations, Int. J. of Therm. Sci. 109 (2016) 81–89. DOI: https://doi.org/10.1016/j.ijthermalsci.2016.05.030.

[31]   Y. Dong, B.Y. Cao, Z.Y. Guo, Ballistic-diffusive phonon transport and size induced anisotropy of thermal conductivity of silicon nanofilms, Physica E: Low-dimensional Systems and Nanostructures 66 (2015) 1–6. DOI: https://doi.org/10.1016/j.physe.2014.09.011.

[32]   S. Hamian, T. Yamada, M. Faghri, K. Park, Finite element analysis of transient ballistic-diffusive phonon heat transport in two-dimensional domains, Int. J. of Heat and Mass Trans. 80 (2015) 781–788. DOI: https://doi.org/10.1016/j.ijheatmasstransfer.2014.09.073.

[33]   Y.C. Hua, B.Y. Cao, Ballistic-diffusive heat conduction in multiply-constrained nanostructures, Int. J. of Therm. Sci. 101 (2016) 126–132. DOI: https://doi.org/10.1016/j.ijthermalsci.2015.10.037.

[34]   Y. Zhang, W. Ye, Modified ballistic-diffusive equations for transient non-continuum heat condition, Int. J. of Heat and Mass Trans. 83 (2015) 51–63. DOI: https://doi.org/10.1016/j.ijheatmasstransfer.2014.11.020.

[35]   M. Xu, H. Hu, A ballistic-diffusive heat conduction model extracted from Boltzmann transport equation, Philos. Trans. Roy. Soc. London A, Math. Phys. Sci. 467 (2011) 1851–1864. DOI: 10.1098/rspa.2010.0611.

[36]   M. Asheghi, Y.K. Leung, S.S. Wong, K.E. Goodson, Phonon-boundary scattering in thin silicon layers, App. Phys. Lett. 71 (13) (1997) 1798–1800. DOI: https://doi.org/10.1063/1.119402.

[37]   Y.S. Ju, K.E. Goodson, Phonons scattering in silicon films thickness of order 100 nm, App. Phys. Lett. 74 (20) (1999) 3005–3007.DOI: https://doi.org/10.1063/1.123994.

[38]   W. Liu, M. Asheghi, Phonon boundary scattering in ultra-thin single crystal silicon layers, Appl. Phys. Lett. 84 (19) (2004) 3819–3821. DOI: https://doi.org/10.1063/1.1741039.

[39]   D. Olfe, A modification of the differential approximation for radiative transfer, AIAA J. 5 (4) (1967) 638–643. DOI: https://doi.org/10.2514/3.4041.

[40]   F. Nasri, M.F. Ben Aissa, M.H. Gazzah, H. Belmabrouk, 3D thermal conduction in nanoscale Tri-Gate MOSFET based on single-phase-lag model, Appl. Therm. Eng. 91 (2015) 647–653. DOI: https://doi.org/10.1016/j.applthermaleng.2015.08.045.

[41]   Y.C. Hua, B.Y. Cao, The effective thermal conductivity of ballistic-diffusive heat conduction in nanostructures with internal heat source, Int. J. of Heat and Mass Trans. 92 (2016) 995–1003. DOI: https://doi.org/10.1016/j.ijheatmasstransfer.2015.09.068.

[42]   C. Tomas, A. Cantarero, A.F. Lopeandia, F.X. Alvarez, Enhancing of optic phonon contribution in hydrodynamic phonon transport, J. Appl. Phys. 118 (13) (2015) 134305. DOI: https://doi.org/10.1063/1.4932034.

[43]   S. Kwon, M.C. Wingert, J. Zheng, J. Xiang, R. Chen, Thermal transport in Si and Ge nanostructures in the 'confinement' regime, Nanoscale, 8 (27) (2016) 13155–13167. DOI: 10.1039/C6NR03634A.

[44]   M. Calvo-Schwarzwälder, M.G. Hennessy, P. Torres, T.G. Myers, F.X. Alvarez, A slip-based model for the size-dependent effective thermal conductivity of nanowires, Int. Comm. Int. J. of Heat and Mass Trans. 91 (2018) 57–63. DOI: https://doi.org/10.1016/j.icheatmasstransfer.2017.11.013.

[45]   A. Sellito, l. Carlomango, D. Jou, Two-dimensional phonon hydrodynamics in narrow strips, Philos. Trans. Roy. Soc. London A, Math. Phys. Sci. 471 (2015) 2182. DOI: 10.1098/rspa.2015.0376.

[46]   C. Y. Zhu, W. You, Z. Y. Li, Nonlocal effects and slip heat flow in nanolayers, Sci. Rep. 7 (2017) 9568. DOI: 10.1038/s41598-017-10416-9.

[47]   S. Ghosh, W. Bao, D.L. Nika, S. Subrina, E.P. Pokatilov, C. Ning, A.A. Balandin, Dimensional crossover of thermal transport in few-layer graphene, Nature Mat. 9 (2010) 555–558. DOI: 10.1038/nmat2753.

[48]   Y. Guo, M. Wang, Heat transport in two-dimensional materials by directly solving the phonon Boltzmann equation under Callaway's dual relaxation model, Phys. Rev. B, 96 (2017) 134312. DOI: 10.1103/PhysRevB.96.134312.

[49]   H. Rezgui, F. Nasri, M.F. Ben Aissa, A.A. Guizani, Study of heat dissipation mechanism in nanoscale MOSFETs using BDE model, In: C. Ravariu, editor. Green Electronics, IntechOpen. (2018). DOI: https://dx.doi.org/10.5772/intechopen.75595.

[50]   S.L. Sobolev, Discrete space-time model for heat conduction: Application to size dependent thermal conductivity in nano-films, Int. J. of Heat and Mass Trans. 108 (2017) 933–939. DOI: https://doi.org/10.1016/j.ijheatmasstransfer.2016.12.051.

[51]   K.R. Hahn, M. Puligheddu, L. Colombo, Thermal boundary resistance at Si/Ge interfaces determined by approach-to-equilibrium molecular dynamics simulations, Phys. Rev. B 91 (2015) 195313. DOI: 10.1103/PhysRevB.91.195313.

[52]   F.X. Alvarez, D. Jou, Boundary conditions and evolution of ballistic heat transport, J. Heat Trans. 132 (1) (2010) 012404. DOI: 10.1115/1.3156785.

[53]   D.L. Nika, A.S. Askerov, A.A. Balandin, Anomalous Size Dependence of the thermal conductivity of Graphene Ribbons, Nano Lett. 12 (6) (2012) 3238–3244. DOI: 10.1021/nl301230g.

[54]   K. Fic, A. Platek, J. Piwek, E. Frackowiak, Sustainable materials for electrochemical capacitors, Materials Today (21) (4) (2018) 437–454. DOI: https://doi.org/10.1016/j.mattod.2018.03.005.

[55]   V.P. Pham, H.S. Jang, D. Whang, J.Y. Choi, Direct growth of graphene on rigid and flexible substrates: progress, applications and challenges. Chem. Soc. Rev. 46 (20) (2017) 6270–6300. DOI: 10.1039/c7cs00224f.

[56]   C. Zhu, D. Du, Y. Lin, Graphene-like 2D nanomaterial-based biointerfaces for biosensing applications, Biosensors and Bioelectronics, 89 (2017) 43–55. DOI: https://doi.org/10.1016/j.bios.2016.06.045.

[57]   Y. Guo, M. Wang, Phonon hydrodynamics and its applications in nanoscale heat transport, Phys. Rep. 595 (2015) 1–44. DOI: https://doi.org/10.1016/j.physrep.2015.07.003.

Table

Table I: Thermal properties of Silicon and Germanium materials.

Symbol	V (m s^{-1})	K (Wm^{-1} K^{-1})	C (J m^{-3} k^{-1})	Mean free path (nm)	Kn	References
Si	1804	145.6	0.93 x 10^6	260.4	13	[22]
Ge	1042	60	0.87 x 10^6	198.6	9.93	[22]

Figure captions
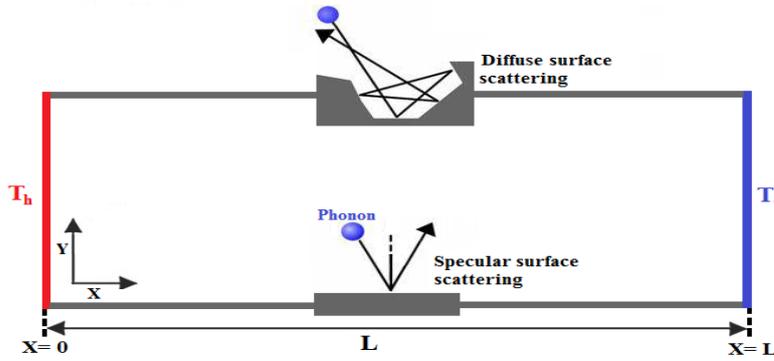
FIG. 1. Schematic illustration of phonon-surface scattering.
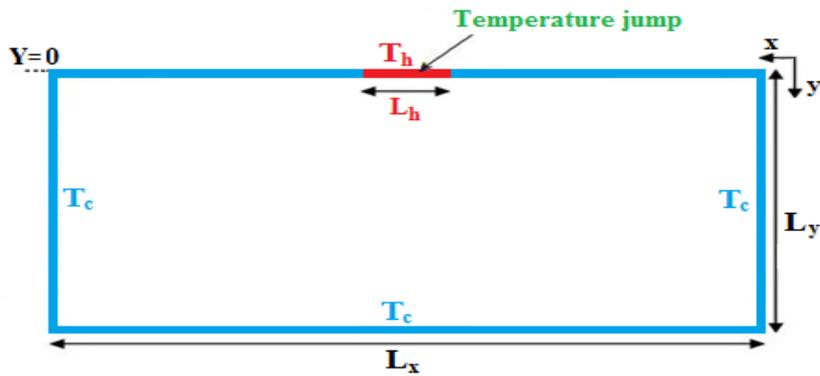
FIG. 2. Boundary conditions of the 2D problem.
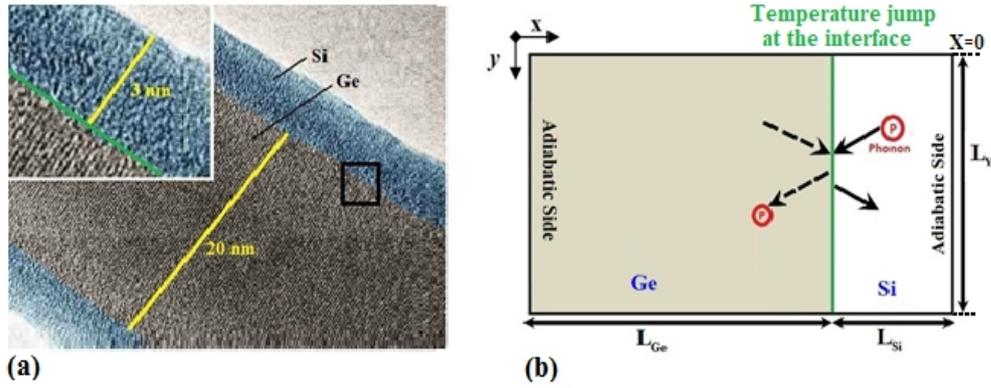
FIG. 3. (a) Nanofilm (Si) on substrate (Ge) [14], (b) Mechanism of phonon scattering at the interface Ge/Si.
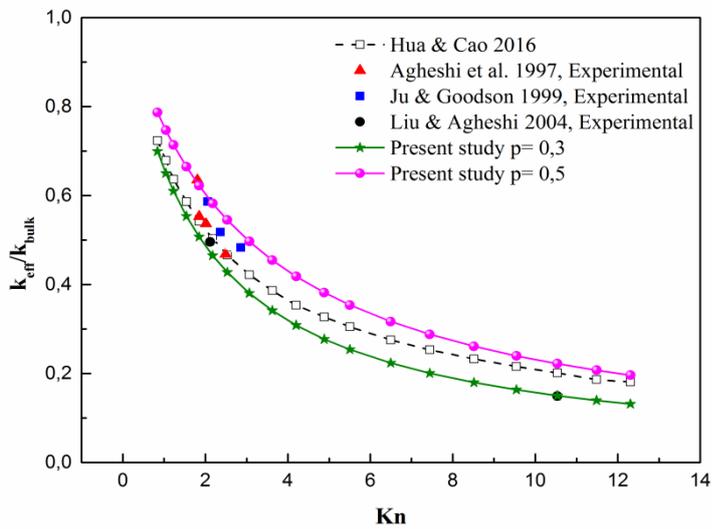

FIG. 4. Comparison of thermal conductivity for Silicon thin films. Solid lines represent the theoretical model given by Eq. (20). Dashed line correspond to Ref. [33]. The symbols denote the experimental results obtained in [36–38].
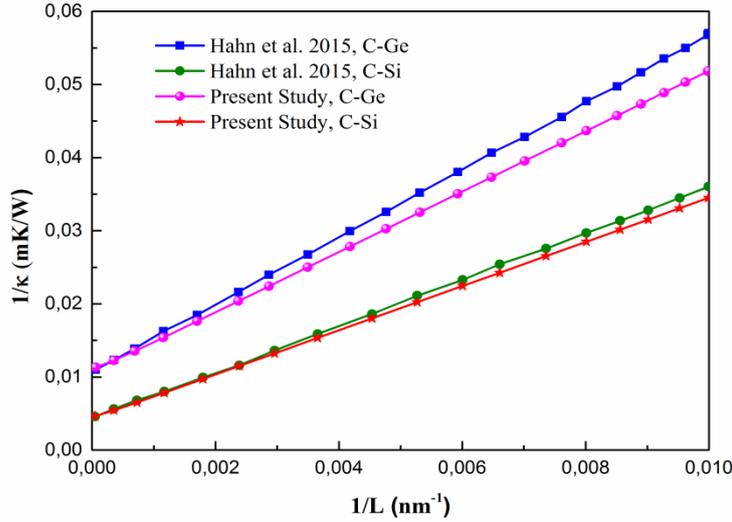
FIG. 5. Inverse of thermal conductivity as a function of the inverse length of crystalline c-Si (κ= 233.4 $Wm^{-1}k^{-1}$) and c-Ge (κ= 93.3 $Wm^{-1}k^{-1}$). The solid lines with stars and spheres correspond to Eq. (20) with p= 0.1. The solid lines with squares and circles represent the data from the literature [51].
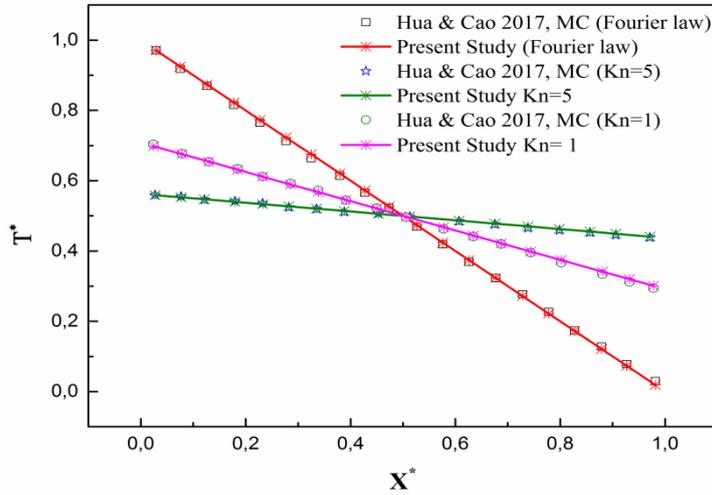

FIG. 6. Dimensionless temperature distribution in nanofilms. The solid lines represent the analytical solution of Eq. (36). Squares, stars and circles denote the Monte Carlo (MC) simulations [22].
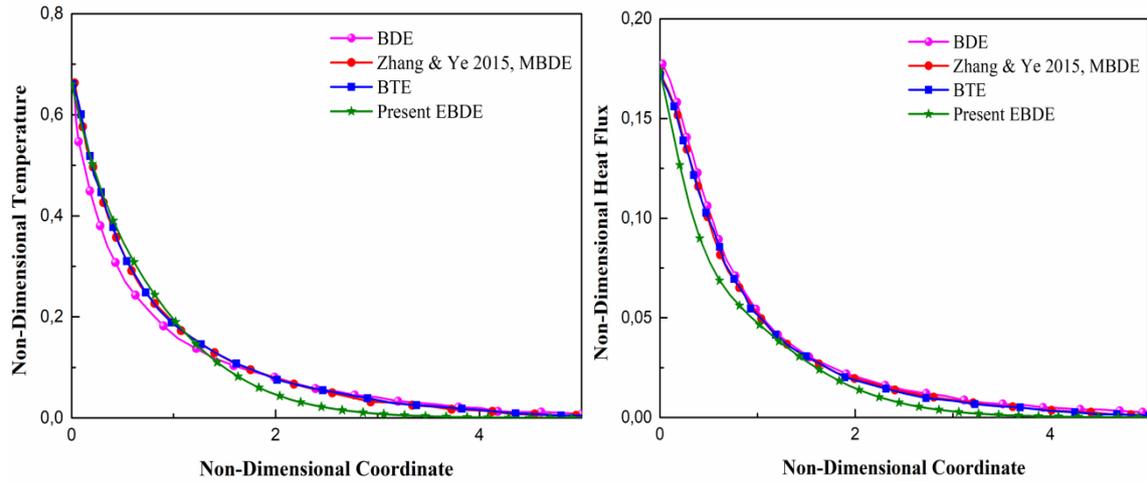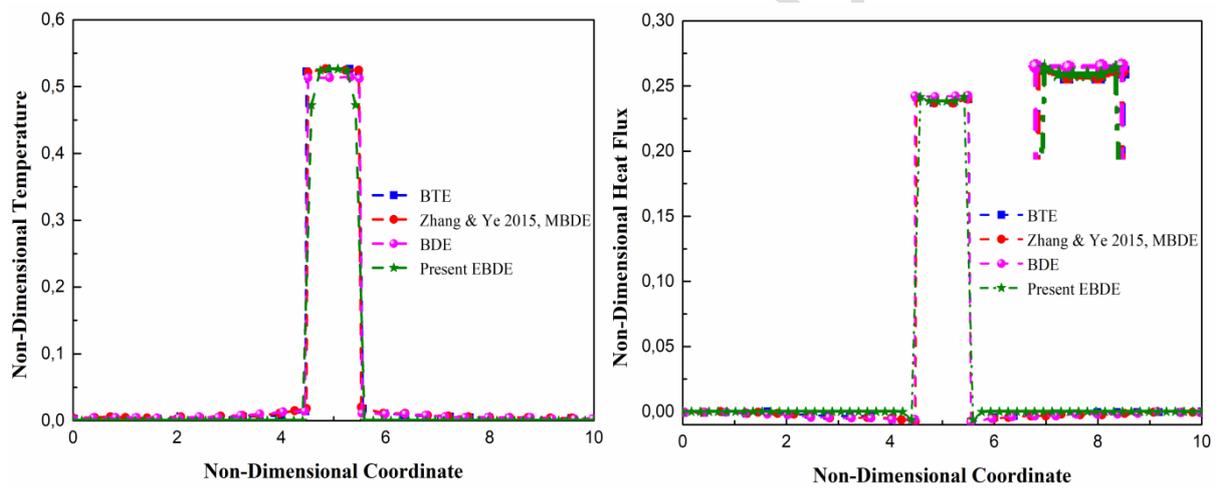
FIG. 7. Temperature and y-direction heat flux evolution along the centerline (X= $L_x/2$) for Kn= 1 at t^*= 10. Solid line and stars represent the enhanced ballistic-diffusive equation (EBDE) correspond to Eq. (22) coupled with the temperature boundary condition given by Eq. (27). Solid line and circles represent the modified ballistic-diffusive equation (MBDE) obtained in Ref. [34].
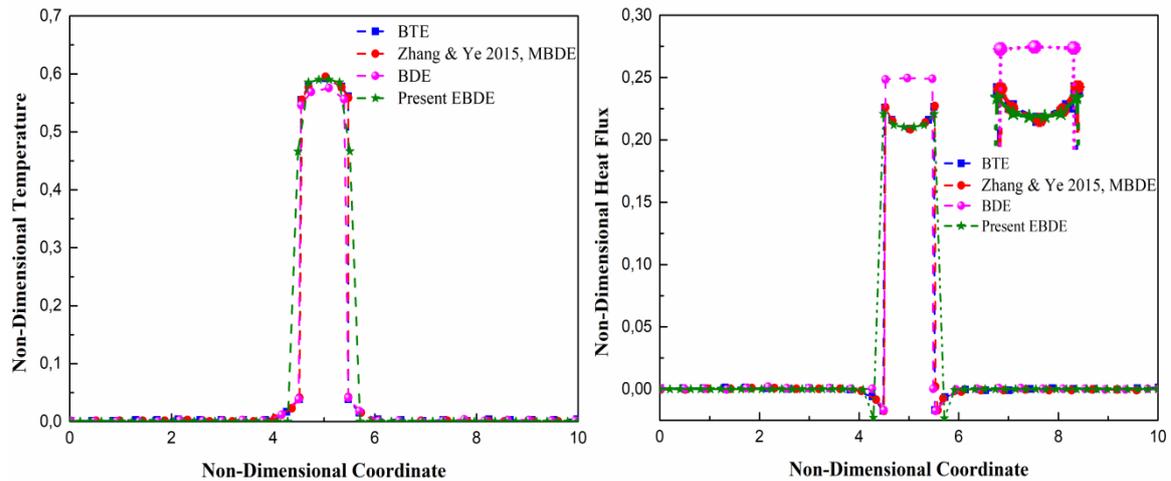
FIG. 8. Temperature and y-direction heat flux evolution along the line y= 0 for Kn= 1 at t^* = 1. Dashed line and spheres represent the original ballistic-diffusive equation (BDE). Dashed line and squares correspond to Boltzmann transport equation (BTE) obtained in Ref. [34].
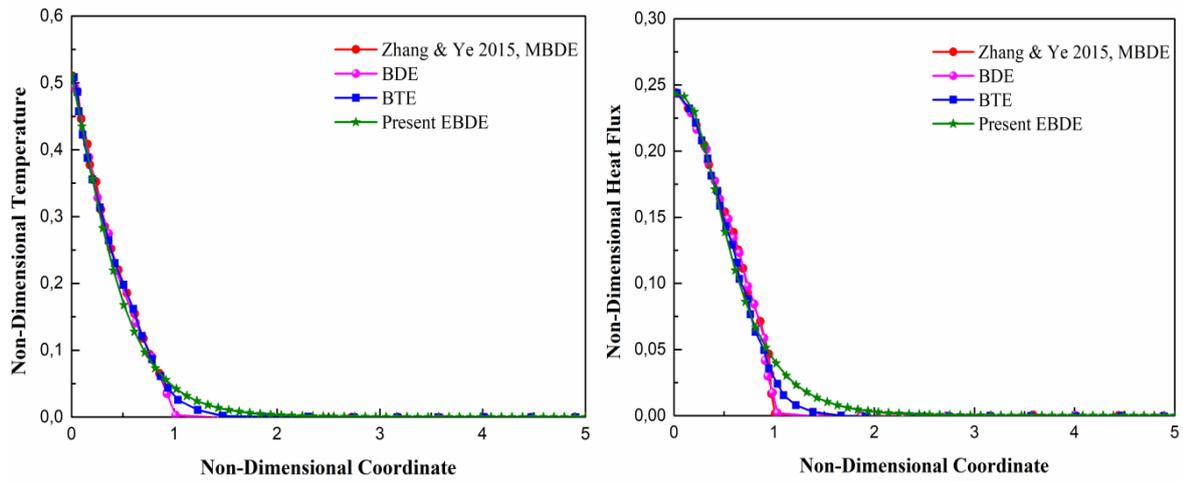
FIG. 9. Temperature and y-direction heat flux evolution along the centerline ($X = L_x/2$) for Kn= 10 at $t^* = 0.1$.

FIG. 10. Temperature and y-direction heat flux evolution along the line y= 0 for Kn= 10 at $t^* = 1$.

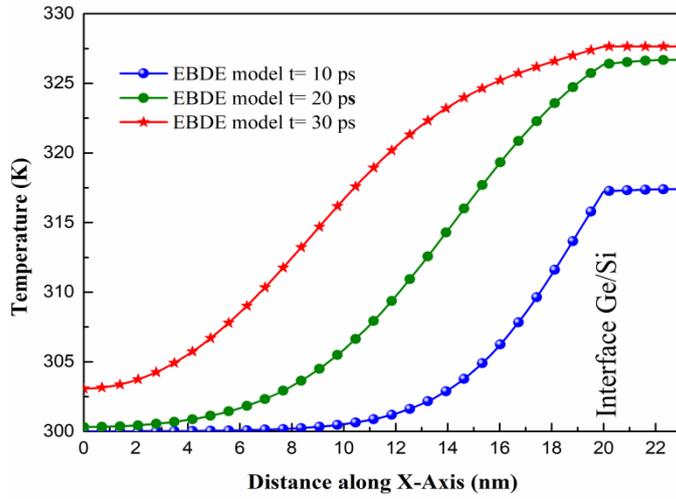**FIG. 11. Temperature evolution across the line X= 0 at t = 10, 20 and 30 ps for p = 0.3. Solid lines represent the EBDE model.**
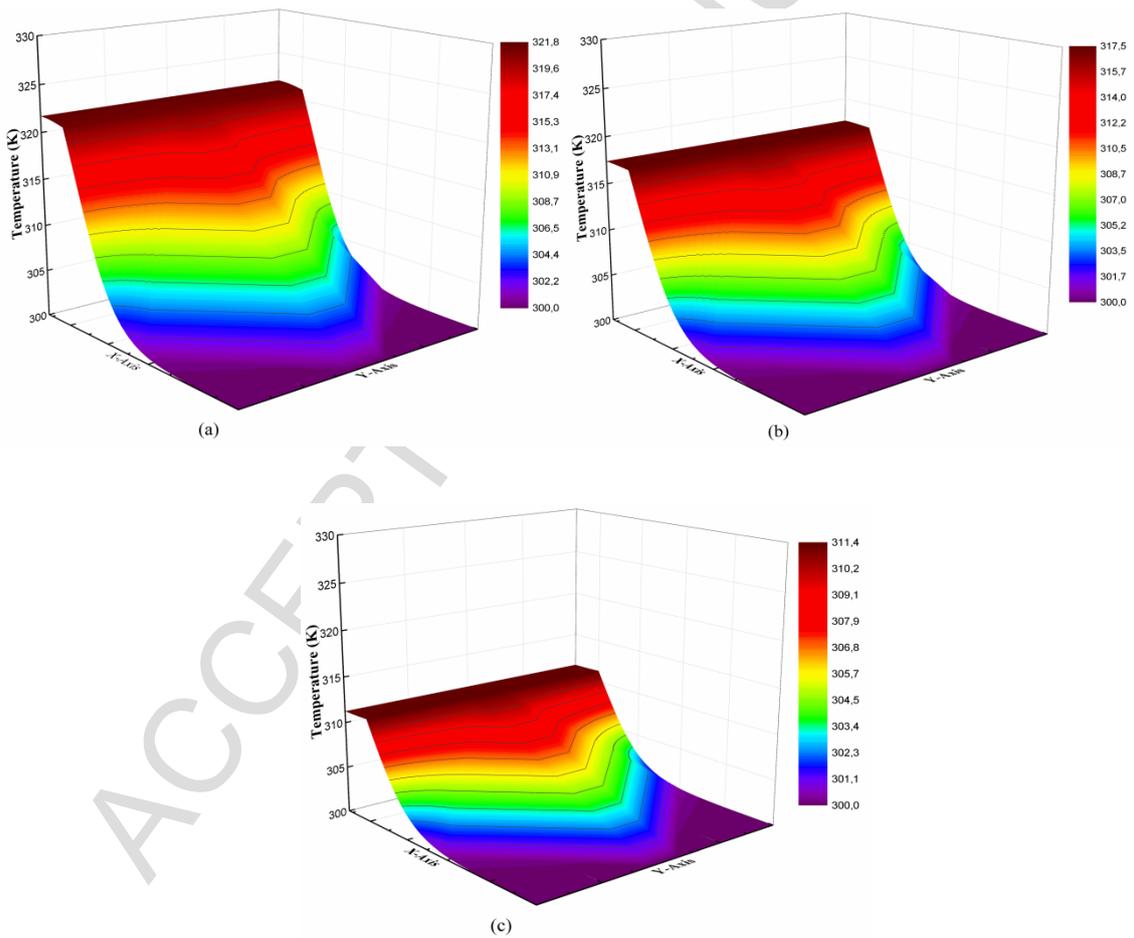

FIG. 12. 2D temperature distribution in X-Y plane using EBDE model at t= 10 ps. (a) p= 0.2, (b) p= 0.3 and (c) p= 0.4.
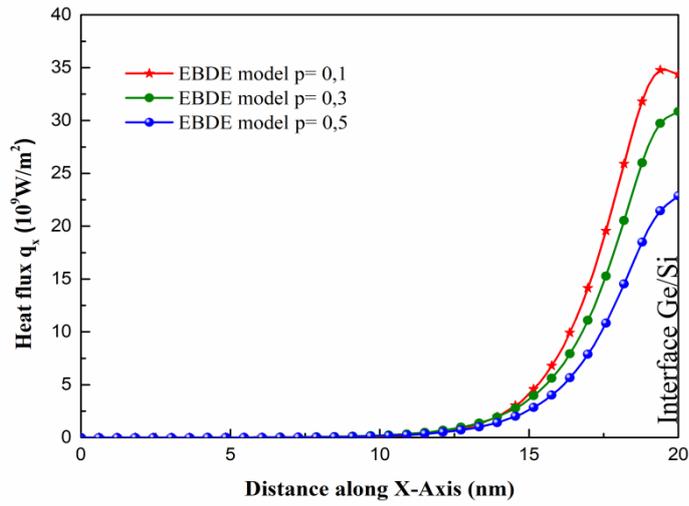
29

FIG. 13. Heat flux evolution across Ge/Si interface at t= 5 ps for different specularity parameter.

Highlights

- An enhanced ballistic-diffusive model is developed for heat transport across the interface scattering between nanomaterials.
- An excellent agreement with experimental results and Monte Carlo simulation.
- Investigation of phonon-surface scattering in nanostructures
- This work help research optimization of interface quality.

Legend:
- Hua & Cao 2016
- Aghesti et al. 1997, Experimental
- Ju & Goodson 1999, Experimental
- Liu & Aghesti 2004, Experimental
- Present study p= 0,3
- Present study p= 0,5

Axes: k_{eff}/k_{bulk} (vertical) vs Kn (horizontal)